

# ANISOTROPY FUNCTION OF A NEW 192-IR BRACHYTHERAPY SOURCE

Rodrigo T. Abreu<sup>1</sup>, Lucas V. Angelocci<sup>1</sup>, Beatriz R. Nogueira<sup>1</sup>, Hamona N. dos Santos<sup>1,2</sup>, Carlos Alberto Zeituni<sup>1</sup> and Maria Elisa C. M. Rostelato<sup>1\*</sup>

<sup>1</sup> Nuclear and Energy Research Institute (IPEN / CNEN - SP)  
Av. Professor Lineu Prestes 2242  
05508-000 São Paulo, SP  
\*elisaros@ipen.br

<sup>2</sup> Federal Institute of Sergipe (IFS)  
R. João Café Filho, 260, Cidade Nova, 49200-000, Estância, SE, Brazil  
hamona.santos@ifs.edu.br

## ABSTRACT

Brachytherapy is a type of radiotherapy that uses radioactive sources (seeds, wires, among others) close to the tumor. Is important to provide a detailed description of seed dosimetry, so only the tumor will be irradiated avoiding unnecessary dose on adjacent organs and structures. To evaluate the dosimetric parameter of the anisotropy function for a new brachytherapy source, this work proposes the use of microcube TLD-100 dosimeters to find the dose rate using the AAPM Task Group 43 protocol (TG-43). The anisotropy function represents dose distribution around the source and has a major role for characterization of a new iridium source being implemented in Brazil. The value of  $D(r,\theta)$  was measured using Solid Water phantoms,  $r$  value being the distance from the geometric center of the source to the position of the dosimeter on the phantom, and  $\theta$  being the angle formed between the longitudinal axis of the source and the line connecting the geometric center to the TLD. Monte Carlo calculations were performed to evaluate the anisotropy function to validate the experimental measurements. For each distance value ( $r$ ), an anisotropy function was plotted (1.0, 2.0, 3.0, 4.0, 5.0, and 10.0 cm). The results obtained with Monte Carlo calculations agreed  $\pm 2\%$  with the experimental values for  $r$  greater than 3.0 cm, so these results show a good distribution of dose around the seed considering the high energy of 192-Ir (average of 380 KeV) and encapsulation thickness.

## 1. INTRODUCTION

Cancer is an uncontrolled development of the cells; the term cancer is used to represent a group of more than 100 illnesses from different locations. According to the International Agency for Research on Cancer (IARC) 2018 World Cancer Report, cancer is one of the major causes of death worldwide. For 2025, more than 20 million of new cases of cancer are estimated [1].

In spite of the ophthalmic cancer not being among the most recurrent kinds of cancer, with an incidence of 3 %, it can induce the loss of the visual function of the eye or even the dead of the patient. That are two types of ordinary intraocular tumors: choroidal melanoma (most common for adults), and retinoblastoma (mostly young children) [2].

Retinoblastoma reaches the retina cells and can spread out causing metastasis, and can also be hereditary. In Brazil this tumor occurs more than the choroidal melanoma [3].

Among the different possible treatments, radiotherapy is an alternative to the enucleation, i.e., the surgical removal of the eye, preventing vision loss and aesthetical problems to the patient, which can also affect self-esteem [4, 5].

Brachytherapy is a type of radiotherapy that uses the radiation sources near to the tumor, changing dose rate, application site, and others parameters such as time of irradiation depending on the tumor size and location [6, 7, 8]. Usually, for brachytherapy, seeds or wires of radioisotopes with low energy of emitted photons are used as sources for the treatment; two examples are the 125-Iodine (ca. 29 keV) and 103-Paladium (ca. 20 keV) [9, 12]. The treatment of retinoblastoma with brachytherapy uses a plaque to allocate the radioactive seeds around the eyeball. The distribution of the seed in those plaques has a major role to the treatment planning and depends on the tumor size and location of the tumor inside the eyeball [4, 9, 10, 11].

In this work the anisotropy function of a new 192-Iridium seed under study in Brazil was carried out using TG-43 protocol parameters.

## 1.1 TG-43 Protocol

In 1995 American Association of Physicians in Medicine (AAPM) created the Task Group 43 to write a protocol for dosimetry based on studies that were conducted since the early 1960s. This protocol is commonly named after the Task Group 43, also known as TG-43, and has the objective of recommending theoretical calculations for brachytherapy sources dosimetry. Since its first version, TG-43 has undergone a major update in 2004, therefore being known as TG-43U1. According to this protocol the absorbed dose rate can be obtained as shown in Equation 1 [12, 13]:

$$\dot{D}(r, \theta) = S_k \cdot \Lambda \cdot \frac{G_L(r, \theta)}{G_L(r_0, \theta_0)} \cdot g_L(r) \cdot F(r, \theta) \quad (1)$$

In this expression,  $S_k$  represents the air-kerma strength and  $\Lambda$  the dose-rate constant, both depending on the radionuclide being used and the very particular geometry of the seed, specially its core and encapsulation. When multiplied, these two values yield the dose rate to reference point, which is located at  $(r_0, \theta_0) = (1, 90^\circ)$ , where  $r$  is the distance from the seed and  $\theta$  the angle from its longitudinal axis. The other three parameters aim to transpose the dose to any other point of interest  $(r, \theta)$ ,  $G_L$  (linear geometry function) altering the dose due to geometry factor,  $g_L$  (radial dose function by a linear source) being used to evaluate the dose along the transversal axis of the seed, affected by its scattering and attenuation, and  $F$  representing the change in dose with the variation of  $\theta$  in any  $r$  of interest, due to the source not being a isotropic emitter.

### 1.1.1 Anisotropy Function

This function describes the dose distribution around the source, which means it verifies the angular variation of the dose rate by the source at different distances from its geometric center. Equation 2 expresses the anisotropy function:

$$F(r, \theta) = \frac{\dot{D}(r, \theta) G_L(r, \theta_0)}{\dot{D}(r, \theta_0) G_L(r, \theta)} \quad (2)$$

The anisotropy function  $F$  essentially evaluates the dose rate to any point normalized by a point equidistant to the source, but lying in the transverse plane ( $\theta_0 = 90^\circ$ ), correcting those values by their respective geometry functions so they do not take into account geometric factors, only variation arising from anisotropy of the source. This way,  $F$  represents only the angular variation contribution to dose fall-off, ignoring geometry effects.

Close to sources there is a strong dose rate gradient, thus making it difficult to measure it precisely at distances less than 5 mm. At very distant points, greater than 10 cm from most sources, the dose is low enough so it can be also difficult to evaluate.  $F$  is expected to decrease with angles near to 0 or 180 degrees, near the source's tips, due to the geometry of the source's core and to its capsule's welds, which usually have greater thickness than the rest of the encapsulation. It is expected to increase in farther distances; in fact, in a distance  $r$  far enough in which the source can be considered a point-source, all values must be close to unity.

## 1.2 <sup>192</sup>Iridium

For this work the source used in the dosimetry was a pure <sup>192</sup>Iridium core sealed in a seed. The core is 3.5 mm in length and has a diameter of 0.6 mm, encapsulated with titanium with a thickness of 0.05 mm. The final seed length is 4.5 mm. Figure 1 represents a schematic model of the seed used for this work with their corresponding measures [14].

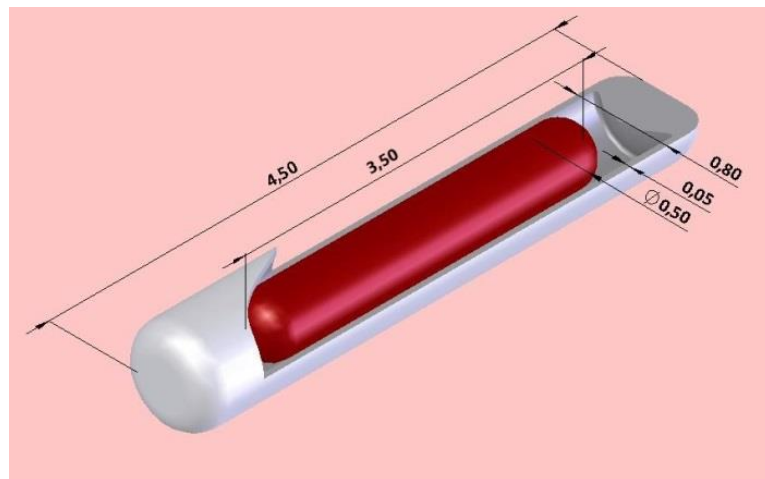


Figure 1 – Schematic model of the <sup>192</sup>Iridium seed (values in mm)

## 1.3 Thermoluminescent Dosimetry

The main objective of thermoluminescent dosimetry (TLD) is to determinate the amount of energy per mass unit of absorbent material that was absorbed in the irradiation process.

Materials used in thermoluminescent dosimetry have a unique property of emitting light when heated proportional to the energy absorbed due to previous irradiation [15, 16].

The mass and density of the absorbent material has a huge influence on the dosimetry. The general density of a patient is around 1 g/cm<sup>3</sup>, due to high amount of soft tissue, and therefore of water, on the body. Considering this, water would be a good material to emulate human body, but the dosimetry in water using TLDs is impracticable for brachytherapy due the decrease of the dosimeters' position accuracy. A solid phantom made of a plastic material avoid this kind of problem, since it can be previously machined to have holes defined for the TLDs position [17, 18, 19].

## **1.4 Monte Carlo Simulation**

The Monte Carlo method is a statistical method that enables the simulation of particles by a random number generator to reproduce mathematically a physical model representing the real system. This method describes individually a set of particles of interest from their initial coordinate in which they are transported following nuclear data gathered by the code until they are absorbed or leave the system.

For Medical Physics field, especially in dosimetry, Monte Carlo method is used to calculate absorbed dose to a single structure, dose distribution in a certain region, shielding, among other parameters that are relevant to the clinical area [20].

Monte Carlo was used in this work to certify the experimental results of anisotropy function following the TG-43 protocol, which recommends it.

## **2. MATERIALS AND METHODS**

The experimental development of this work was performed at the Radiation Technology Center (CETER) in Nuclear and Energy Research Institute (IPEN/CNEN-SP).

### **2.1 Materials**

The materials used to perform the dosimetry were:

- CAPINTEC® model CRC-15W;
- 192-Iridium seeds produced by Radiotherapy Sources Production laboratory under the coordination of PhD. Maria Elisa C. M. Rostelato in IPEN/CNEN-SP;
- Real water phantom RW1 (PTW®) of polystyrene (PS) for anisotropy function analysis;
- Thermoluminescent microcubes of lithium fluoride doped with magnesium and titanium (TLD-100) purchased from Harshaw;
- 3500 Thermo-Harshaw thermoluminescent reader;
- WinREMS software for data acquisition;
- MCNP4C (Monte Carlo N-Particle Radiation Transport Code version 4C).

## 2.2 Methods

### 2.2.1 Experimental

Experimental data of  $^{192}\text{Ir}$ -Iridium dosimetry were obtained through the following steps:

- Source activity measure and correction

To perform the correction of the activity of the source along the time, some nuclear data of  $^{192}\text{Ir}$ -Iridium was necessary. This isotope has a half-life of 73.83 days (1771.92 hours) and its dose rate constant ( $\lambda$ ) is  $3.91 \times 10^{-04}$  hours [21].

- Measurements using the Solid Water Phantom:

For anisotropy function  $F(r, \theta)$ , the dosimeters were positioned in different angles to evaluate the dose rate. This Phantom has a central spot for the seed and concentric spots for the TLDs as shown in Figure 2.

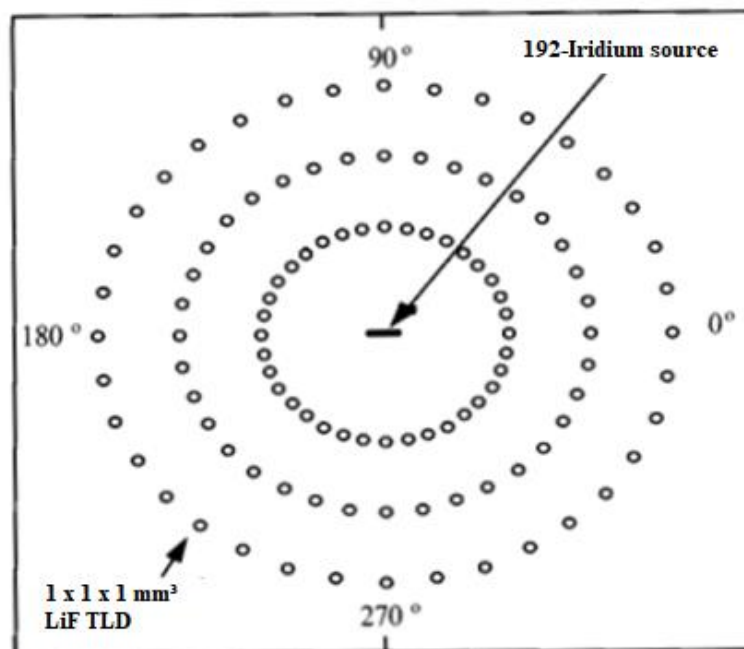


**Figure 2 – Diagram of the Solid Water Phantom RW1 for anisotropy function measurements**

Measurements of the anisotropy function were made for six distances (1 cm, 2 cm, 3 cm, 4 cm, 5 cm, and 10 cm) from the geometric center of the iridium source.

- Correction of the source activity values:

Once it was necessary to perform many measurements in different positions, the period for acquisition of the irradiated TLDs took a long time, so the activity of the source needed to be corrected following the Equation 3.

$$A_f = A_i \cdot e^{-\lambda t} \quad (3)$$

Where  $A_i$  is the activity at the beginning of measurement,  $A_f$  is the activity at the end of it,  $\lambda$  is the disintegration constant, and  $t$  is the measurement time. After that, the value of activity correction  $C_a$  is given by the Equation 4, where  $A_0$  is the activity of the source when it was produced and  $A_{eq}$  is the equivalent activity, i.e., a constant value for activity that yields the same number of photons produced over time  $t$  considering the natural decay of the source.

$$C_a = \frac{A_0}{A_{eq}} \quad (4)$$

### 2.2.1 Monte Carlo

Two simulations were performed in this work. The first one was to calculate the TG-43 parameters, so the geometries of the source and the sphere surround the seed were defined. For that tally \*F4 with DE/DF card was used, which means dose absorbed in medium was calculated considering average track length and dose to water [22].

As the experimental dosimetry apparatus is associated with the dose deposited in the TLD, is essential to correlate the dose in the dosimeters with the dose calculated in the water. Therefore, the second simulation was used to convert dose-to-TLDs to dose-to-water. This step consolidates the recommendations of the TG-43 that define dosimetry in a homogenous environment encased in water.

## 3. RESULTS AND DISCUSSION

### 3.1 Activity measurements and correction

Table 1 presents the initial activity of 192-Iridium source (day 01) and the subsequent calculated activities (counting the days after this initial measurement), only for days where experimental work was done. The importance of calculating the equivalent activity is noted for longer measurements, as noted for days 34, 42 and 48. For short-timed measurements, the equivalent activity can be approximated as the average of initial and final activities. The activity correction factor increases with the passing of time, representing the increasing need to correct the original value as the source naturally decays.

The measurement time for each day was calculated using preliminary simulations with Monte Carlo method to assure total dose absorbed by the TLD would be in the dosimeter's absorbed dose linear range.

**Table 1 – <sup>192</sup>Iridium seed activity (measured and corrected)**

Time	Initial activity (mCi)	Final activity (mCi)	Equivalent activity (mCi)	Activity correction factor
Day 01	48.80	-	-	-
34 days	35.55	34.89	35.22	1.39
42 days	33.05	32.90	32.98	1.48
48 days	31.20	31.11	31.15	1.57
51 days	30.34	30.28	30.31	1.61
55 days	29.22	29.19	29.20	1.67
62 days	27.34	27.33	27.33	1.79

### 3.2 Anisotropy Function

Figure 3 presents the anisotropy function plots, each point being the average of four measurements taking into different quadrants, at distances of 1, 2, 3, 4, 5 and 10 cm.

For distances of 1 cm and 2 cm, in Figure 3, a dispersed behavior was observed in comparison with the plots of larger distances; this fact may be explained due the shorter irradiation time for smaller distances, which changes the dose rate value, used to calculate the function, therefore increasing its uncertainty. Furthermore, the shorter times of irradiation also increase the experimental uncertainty, as there are no automated steps in the process, and time of assembling and disassembling the experiment were not taken into account.

For larger distances (3, 4, 5, and 10 cm) in Figure 3 it was possible to observe that the experimental results behavior resembles the Monte Carlo method curve but some angles did not fit well to the curve, with a major concern for the points in the angle of 70 and 80 degrees that presented a huge decrease of the value of the function. This may represent an inhomogeneity in the phantom material and therefore a systematic error, or even a problem in the positioning of the seed, due to some inconsistency on the seed spot hole. These considerations will be checked and taken into account on future works.

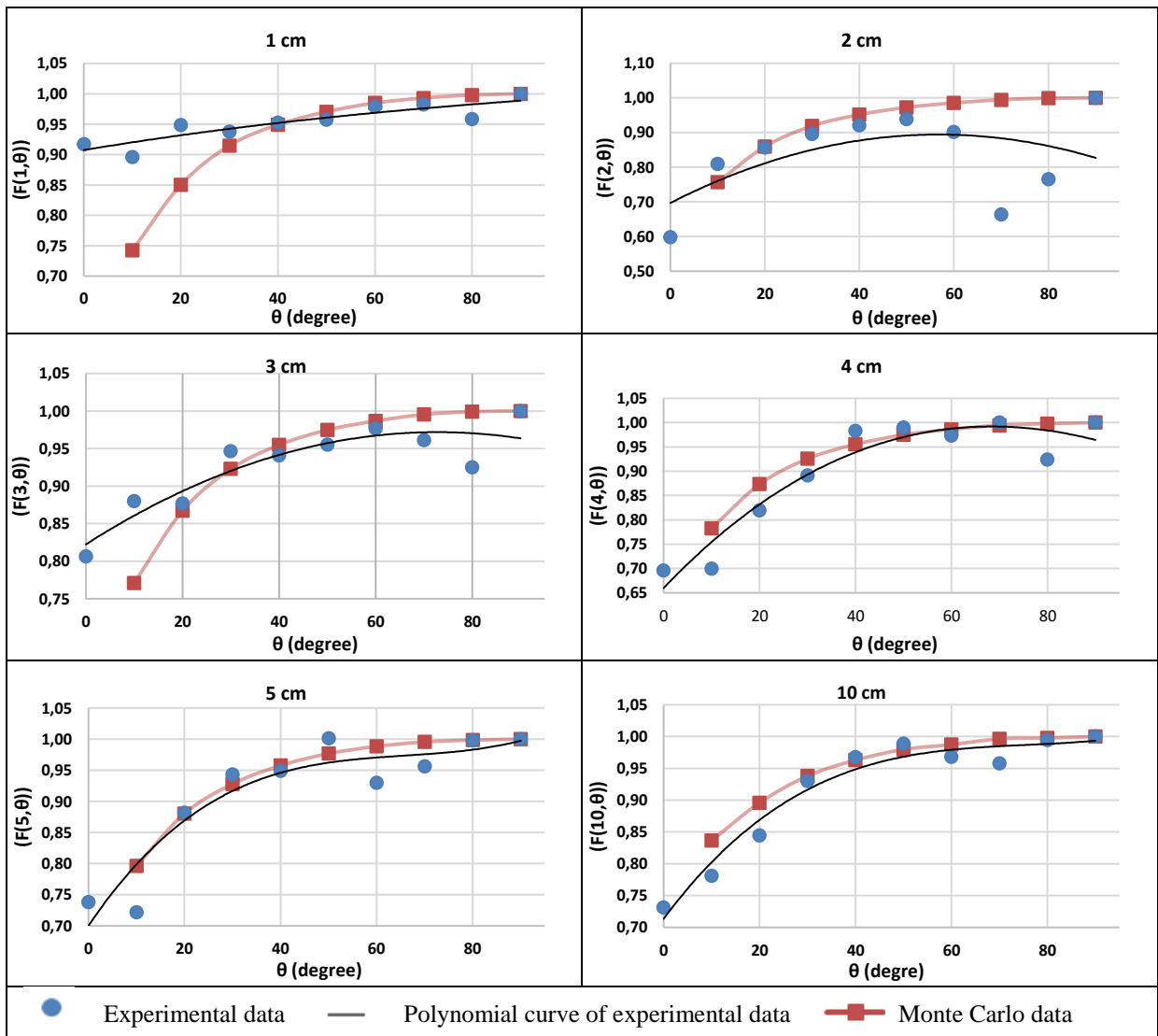


**Figure 3 – Anisotropy function at different distances as a function of the angle**

All plots showed a trend of increasing the value of  $F(r, \theta)$ , as expected due to the increase in the dose rate for angles near 90 degrees. Inconsistencies in the value of continuity of function at some angles may correlate with the fact that the seed has different weld geometry at its ends, which was neglected in this work due to the difficulty of measuring it. Welding of this seed was performed by a laser system that is already used by the research group for the production of brachytherapy seeds, but its effect on dose rate must be further studied [23].

The tables 2 and 3 show the results of the experimental anisotropy function and calculated by Monte Carlo.



**Table 2 – Experimental anisotropy function**

	Angle						
	0,5	1	2	3	4	5	10
<b>0</b>	0,7188	0,9174	0,5982	0,8063	0,6960	0,7380	0,7312
<b>10</b>	0	0,8960	0,8094	0,8799	0,6997	0,7219	0,7813
<b>20</b>	0	0,9486	0,8568	0,8767	0,8193	0,8817	0,8447
<b>30</b>	0,8460	0,9381	0,8963	0,9464	0,8916	0,9432	0,9299
<b>40</b>	0	0,9527	0,9210	0,9411	0,9828	0,9490	0,9677
<b>50</b>	0	0,9574	0,9387	0,9552	0,9899	1,0015	0,9889
<b>60</b>	0,9231	0,9792	0,9019	0,9767	0,9730	0,9297	0,9680
<b>70</b>	0	0,9827	0,6643	0,9610	1,0005	0,9561	0,9576
<b>80</b>	0	0,9584	0,7656	0,9252	0,9238	0,9981	0,9944
<b>90</b>	1	1	1	1	1	1	1

**Table 3 – Anisotropy function by Monte Carlo**

	Angle						
	0,5	1	2	3	4	5	10
<b>0</b>							
<b>10</b>	0,757	0,742	0,757	0,771	0,783	0,796	0,836
<b>20</b>	0,850	0,850	0,859	0,867	0,873	0,880	0,896
<b>30</b>	0,914	0,915	0,919	0,923	0,926	0,928	0,938
<b>40</b>	0,950	0,949	0,952	0,955	0,955	0,958	0,963
<b>50</b>	0,971	0,970	0,973	0,975	0,975	0,977	0,980
<b>60</b>	0,984	0,985	0,985	0,987	0,986	0,988	0,987
<b>70</b>	0,993	0,993	0,994	0,995	0,994	0,995	0,996
<b>80</b>	0,998	0,998	0,999	0,999	0,998	0,999	0,998
<b>90</b>	1,000	1,000	1,000	1,000	1,000	1,000	1,000

Comparing the results of the tables, it can be concluded that the difference between the values found experimentally and the theoretical values calculated by the Monte Carlo method are on average  $\pm 2\%$ . This percentage expresses an adequate agreement between the methods used in this work.

#### 4. CONCLUSIONS

Anisotropy function was calculated following the TG-43 and its correspondent equation (2). The differences observed between experimental and Monte Carlo data may be caused due to some setback that may be happen during the experimental execution, such as the emergence of small crack and fissures in the TLDs, inhomogeneities on the Phantom structure, among others. One example of it is the decrease on the anisotropy function expect result around the angle of 80 degrees. Despite that, it is possible to notice that the anisotropy function for this seed tend to be similar to the one calculated on Monte Carlo simulations, with a good agreement for distances greater than 4 cm.

This work was a preliminary dosimetric study of a 192-Iridium seed Brazilian prototype for ophthalmic brachytherapy application, and the results obtained with this work may contribute for dose distribution analysis around the source.

## ACKNOWLEDGMENTS

The authors would like to thank CNEN, CNPq and CAPES for the scholarships and IAEA for funding fellowships that allowed the work to be made.

This study was financed in part by the Coordenação de Aperfeiçoamento de Pessoal de Nível Superior – Brasil (CAPES) – Finance Code 001.

## REFERENCES

1. Instituto Nacional do Câncer, “Estatísticas do câncer”, <https://www.inca.gov.br/numeros-de-cancer> (2018).
2. K. R. Patel, R. S. Prabhu, J. M. Switchenko, M. Chowdhary, C. Craven; P. Mendoza, H. Danish, H. E. Grossniklaus, T. M. SR Aaberg, T. JR Aaberg, S. Reddy, E. Butker, C. Bergstrom, I. R. Crocker, “Visual acuity, oncologic, and toxicity outcomes with 103 Pd vs. 125 I plaque treatment for choroidal melanoma,” *Brachytherapy*, v. **16**, n. 3, pp. 646-653 (2017).
3. K. C. B. Ribeiro, C. B. G. Antoneli, “Trends in eye cancer mortality among children, 1980 – 2002,” *Pediatr Blood Cancer*, v. **48**, pp. 296-305 (2007).
4. A. P. Mourão, T. P. R. Campos, “Dosimetry on ocular brachytherapy with I-125 ophthalmologic ROPES and COMS plaques,” *International Nuclear Atlantic Conference*, Rio de Janeiro, 2009.
5. P. T. Finger, L. B. Tena, E. Semenova, P. Aridgides, W. H. Choi, “Extrascleral extension of choroidal melanoma: Post-Enucleation high-dose-rate interstitial brachytherapy of the orbit,” *Brachytherapy*, v. **13**, n. 3, pp. 275-280.
6. K. P. Hermann, W. Alberti, P. Tabor, B. Pothmann, S. Divoux, D. Harder, “Solid phantom material for the dosimetry of iodine-125 seed ophthalmic plaques,” *International Journal of Radiation Oncology Biology Physics*, v. **26**, n. 5, pp. 897-901 (1993).
7. E. Okuno, E. Yoshimura, *Física das Radiações*, Oficina de Textos (2010).
8. M. E. C. M. Rostelato, *Preparação de fontes de irídio-192 para uso em braquiterapia*, Dissertation (Master in Science in the area of Nuclear Technology - Applications) IPEN. São Paulo (1997).
9. F. R. Mattos, *Estudo e Desenvolvimento de uma semente de Iridio-192 para aplicação em câncer oftalmológico*, Dissertation (Master in Science in the area of Nuclear Technology - Applications) IPEN. São Paulo (2013).
10. G. Luxton, M. A. Astrahan, P. E. Liggett, D. L. Neblett, D. M. Cohen, Z. Petrovich, “Dosimetric calculations and measurements of gold plaque ophthalmic irradiators using iridium-192 and iodine-125 seeds,” *International Journal of Radiation Oncology Biology Physics*, v. **15**, n. 1, pp. 167-176 (1988).
11. F. Valcarcel, S. Valverde, H. Cárdenes; C. Cajigal, A. De La Torre, R. Magallón, C. Regueiro, J. L. Encinas, G. Aragón, “Episcleral iridium-192 wire therapy for choroidal melanoma,” *International Journal of Radiation Oncology Biology Physics*, v. **30**, pp. 1091-1097 (1994).

12. R. Nath, "Dosimetry of interstitial brachytherapy sources: recommendations of the AAPM Radiation Therapy Committee Task Group No. 43". *Medical physics*, v. **22**, n. 2, pp. 209-234 (1995).
13. M. J. Rivard, B.M. Coursey, L. A. Dewerd, W. F. Hanson, M. S. Huq, G. S. Ibbott, M. G. Mitch, R. Nath, J. F. Williamson, "Update of AAPM Task Group No. 43 Report: A revised AAPM protocol for brachytherapy dose calculations," *Medical physics*, v. **31**, n. 3, pp. 633-674 (2004).
14. C. D. Souza, *Comparação entre métodos de fixação do iodo radioativo em substrato de prata para a confecção de fontes utilizadas em braquiterapia*, Dissertation (Master in Science in the area of Nuclear Technology - Applications) IPEN. São Paulo (2012).
15. H. E. Johns, *The Physics of Radiology*, Charles C Thomas (1983).
16. J. R. Cameron, N. Suntharalingam, G. N. Kenney, *Thermoluminescent Dosimetry* (1968).
17. IAEA TRS-398, *Absorbed Dose Determination in External Beam Radioterapy: An International Code of Absorbed Dose to Water*, Vienna (2000).
18. D. R. White, I. J. Wilson, J. A. Booz, J. J. A. Spokas, R. V. Griffith, "ICRU Report 44 - Tissue Substitutes in Radiation Dosimetry and Measurements," *Journal of the International Commission on Radiation Units and Measurements in Radiation Dosimetry and Measurements*, v. **23**, n. 1 (1989).
19. A. S. Meigooni, J. A. Meli, R. Nath, "A comparison of solid phantoms with water for dosimetry of 125I brachytherapy sources," *Medical Physics*, v. **15**, n. 5, pp. 695-701 (1988).
20. A. Moutsatsos, E. Pantelis, P. Papagiannis, D. Baltas, "Experimental determination of the Task Group-43 dosimetric parameters of the new I25. S17plus 125I brachytherapy source," *Brachytherapy*, v. **13**, n. 6, pp. 618-626 (2014).
21. M. P. Unterweger, D. D. Hoppes, F. J. Schima, "New and revised half-life measurements results," *Nuclear Instruments and Methods in Physics Research Section A: Accelerators, Spectrometers, Detectors and Associated Equipment*, v. **312**, n. 1-2, pp. 349-352 (1992).
22. J. K. Shultis, R. E. Faw, *An MCNP primer*, pp. 1-42 (2011).
23. A. FEHER, *Estudo e desenvolvimento de um sistema de soldagem a laser ND: YAG para a produção de sementes de Iodo-125 utilizadas em braquiterapia*, Thesis (PhD in Sciences in the area of Nuclear Technology - Applications) IPEN. São Paulo (2014).